AIAA JOURNAL
Vol. 35, No. 7, July 1997

# Screech Tones of Supersonic Jets from Bevelled Rectangular Nozzles

Christopher K. W. Tam* and Hao Shen†
*Florida State University, Tallahassee, Florida 32306-3027*
and
Ganesh Raman‡
*NYMA Inc., Brook Park, Ohio 44142*

**It is known experimentally that an imperfectly expanded rectangular jet from a thin-lip convergent nozzle emits only a single dominant screech tone. The frequency of the screech tone decreases continuously with an increase in jet Mach number. However, for a supersonic jet issued from a bevelled nozzle or a convergent-divergent nozzle with straight side walls, the shock cell structure and the screech frequency pattern are fairly complicated and have not been predicted before. It is shown that the shock cell structures of these jets can be decomposed into waveguide modes of the jet flow. The screech frequencies are related to the higher-order waveguide modes following the weakest link screech tone theory. The measured screech frequencies are found to compare well with the predicted screech frequency curves.**

## I. Introduction

RECENTLY, there is a renewed interest in the possible application of rectangular jets to future generation aircraft propulsive system. Rectangular jets are regarded to have the potential for jet mixing enhancement and noise reduction. Furthermore, they are known to have thrust vectoring capability.

When operating at imperfectly expanded conditions, a supersonic rectangular jet emits discrete frequency screech tones. Earlier, these tones have been studied experimentally by Powell,[1] Hammitt,[2] Krothapalli et al.,[3] and others. During the last few years, screech tones have been the subject of several research studies.[4–10] In the most recent work of Raman,[10] bevelled rectangular nozzles were used. By shaping the nozzle exit geometry, it was hoped that there could be additional noise and mixing benefits.

The shock cell structure of an imperfectly expanded rectangular jet with a straight exit is quite complicated. Figure 1 shows the spark schlieren image of the top view of such a shock cell structure associated with an aspect ratio 5 convergent rectangular nozzle. The jet Mach number is 1.4. If, instead of a regular straight exit nozzle, a bevelled nozzle is used, the shock cell structure becomes even more complex. This can be seen in Fig. 2. The jet Mach number is again 1.4. The shock cell structure is not only highly three dimensional but also contains many fine-scale features. There is asymmetry about the centerline of the jet. However, the initial shock cell spacing appears to be about the same as that of a jet with a straight exit. Overall the shock cell structure is still quasiperiodic.

It was observed experimentally, since the pioneering work of Powell,[1] that a rectangular jet from a thin-lip convergent nozzle emits only one dominant screech tone (and its harmonics). Over the years, this finding has been confirmed by all subsequent investigators. Figure 3 shows a typical variation of the screech frequency with increase in jet Mach number. The data[10] are for a jet issued from an aspect ratio 5 convergent nozzle with exit dimensions $6.58 \times 1.32$ cm. In contrast to the simplicity of the regular straight nozzle case, the tone frequency Mach number relation for rectangular jets from bevelled nozzles is highly complicated.[10] Observations revealed that it is possible for a jet to emit more than one dominant screech tone simultaneously. A closer inspection of the data indicates that even sudden frequency jumps can occur. The physical mechanism responsible for this screech tone frequency pattern is not well understood.

The present investigation seeks a physical explanation of the observed screech frequency jet Mach number relation for bevelled rectangular nozzles. Both convergent and convergent-divergent nozzles are considered. Obviously, the screech frequency must be closely related to the shock cell structure in the jet plume. For this reason, a linear model shock cell structure of a supersonic jet from a bevelled rectangular nozzle will first be established. The use of a linear shock cell model for screech frequency and broadband shock associated noise prediction is not new. Such a model has been used successfully in Refs. 11–15. As in previous works, the present shock cell structure model is formed by a superposition of the waveguide modes of the jet flow. For screech frequency prediction, attention is focused on the lower-order modes.

It is known that screech tones are generated by a feedback loop.[1,16] According to the weakest-link theory,[17] the feedback loop is driven by the large-scale instability waves of the jet flow. The instability waves are excited at the nozzle exit region near the nozzle lip, where the jet is most receptive to external excitation, by acoustic disturbances. The excited instability waves extract energy from the mean flow and grow quickly as they propagate downstream. After propagating a distance of about three to four shock cells, they, having grown to relatively high amplitudes, interact strongly with the shock cell structure. As a result of the interaction, strong acoustic waves are generated. Part of the acoustic waves propagate upstream outside the jet. Upon impinging on the jet near the nozzle lip region, the acoustic disturbances excite the shear layer, thus generating new instability waves. In this way, the feedback loop is closed. Tam et al.[17] observed that the acoustic waves that radiated to the nozzle lip region were confined to a narrow frequency band if they were generated by the interaction between the large-scale instability waves and the quasiperiodic shock cell structure of a supersonic jet. The band is centered around frequency $f_p$ given by

$$f_p = \frac{u_c \kappa}{2\pi[1 + (u_c/a_\infty)]} \tag{1}$$

where $u_c$ is the convection or phase velocity of the instability waves, $a_\infty$ is the ambient sound speed, and $\kappa$ is the wave number of the shock cell structure. The weakest link of the feedback loop is the process of excitation of the large-scale instability waves by the feedback acoustic waves near the nozzle lip. To maintain the loop, the screech tone frequency must fall within the narrow band centered around $f_p$

Received Sept. 9, 1996; presented as Paper 97-0143 at the AIAA 35th Aerospace Sciences Meeting, Reno, NV, Jan. 6–10, 1997; revision received March 17, 1997; accepted for publication April 1, 1997. Copyright © 1997 by the authors. Published by the American Institute of Aeronautics and Astronautics, Inc., with permission.

*Professor, Department of Mathematics. Associate Fellow AIAA.
†Graduate Student, Department of Mathematics.
‡Senior Research Engineer, Experimental Fluid Dynamics Section, NASA Lewis Research Center. Member AIAA.

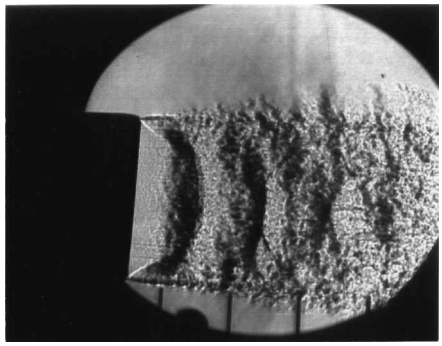

**Fig. 1 Spark schlieren image of the shock cell structure of a Mach 1.4, aspect ratio 5, rectangular jet from a regular convergent nozzle.**

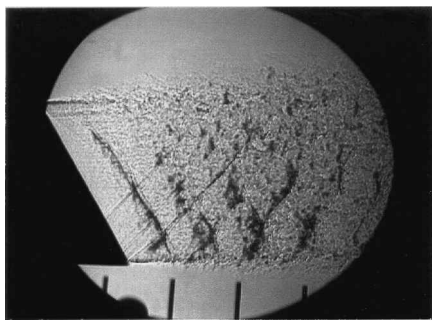

**Fig. 2 Spark schlieren image of the shock cell structure of a Mach 1.4, aspect ratio 5, rectangular jet from a single-bevelled convergent nozzle.**

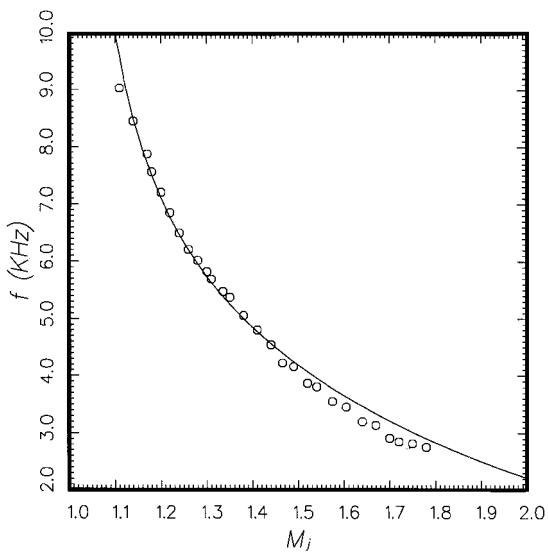


**Fig. 3 Variation of the screech frequency with fully expanded jet Mach number for a supersonic jet from a convergent rectangular nozzle; aspect ratio = 5, regular exit geometry: o measurements[10] and ——, theory.[12]**

given by Eq. (1). Because of this, Eq. (1) offers a good estimate of the screech frequency.

To be able to use Eq. (1) for screech frequency prediction, $u_c$ and $\kappa$ must first be found. For circular jets, Harper-Bourne and Fisher[18] measured experimentally that $u_c \simeq 0.7u_j$ ($u_j$ is the jet speed). However, for rectangular jets Tam and Reddy[19] found it was more appropriate to use a lower convection velocity. They recommended

$$u_c \simeq 0.55u_j \tag{2}$$

In this work, formula (2) will be used throughout.

By means of a vortex sheet jet model, Tam[12] found that the pressure distribution $p$ associated with the shock cell structure of a rectangular jet can be decomposed into waveguide modes with eigenfunctions (mode shape) $\phi_{nm}(y, z)$ and wave number $k_{nm}$. With respect to a Cartesian coordinate system shown in Fig. 4 for a jet

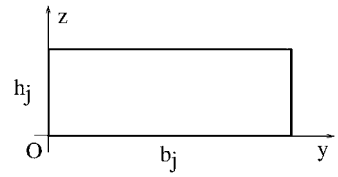


**Fig. 4 Coordinates used to calculate the shock cell structure of rectangular jets.**

with fully expanded width $b_j$ and height $h_j$, the pressure distribution $p$ may be represented by an expansion in the form

$$p(x, y, z) = \sum_{n=1}^{\infty}\sum_{m=1}^{\infty} \phi_{nm}(y, z)[A_{nm}\cos(k_{nm}x) + B_{nm}\sin(k_{nm}x)] \tag{3}$$

where

$$\phi_{nm}(y, z) = \sin(n\pi y/b_j)\sin(m\pi z/h_j) \tag{4}$$

$$k_{nm} = \left(\frac{n^2}{b_j^2} + \frac{m^2}{h_j^2}\right)^{\frac{1}{2}} \frac{\pi}{(M_j^2 - 1)^{\frac{1}{2}}} \tag{5}$$

The coefficients $A_{nm}$ and $B_{nm}$ are to be determined by the nozzle exit conditions, and $b_j$ and $h_j$ are related to the nozzle exit dimensions $b$ and $h$ by

$$b_j/b = [(A_j/hb) - 1][h/(h + b)] + 1 \tag{6}$$

$$h_j/h = [(A_j/bh) - 1][b/(b + h)] + 1 \tag{7}$$

where

$$\frac{A_j}{bh} = \frac{M_d}{M_j}\left\{\frac{1 + [(\gamma - 1)/2]M_j^2}{1 + [(\gamma - 1)/2]M_d^2}\right\}^{(\gamma+1)/2(\gamma-1)} \tag{8}$$

In Eq. (8), $M_j$ is the fully expanded jet Mach number and $M_d$ is the nozzle design Mach number.

For shock cell mode prediction, the linear model just given is fairly accurate. For instance, the screech frequency of the measured data in Fig. 3 can be predicted by taking $\kappa$ in formula (1) to be the wave number of the lowest waveguide mode ($n = 1$, $m = 1$); i.e.,

$$\kappa = k_{11} = \left(\frac{1}{b_j^2} + \frac{1}{h_j^2}\right)^{\frac{1}{2}} \frac{\pi}{(M_j^2 - 1)^{\frac{1}{2}}} \tag{9}$$

The calculated values form the solid curve. As can be seen, there is good agreement between the measured data and the theoretical prediction over a wide range of Mach numbers.

For bevelled rectangular nozzles, the associated shock cells are necessarily more complicated. To obtain a physical understanding of the screech frequency pattern of these jets, it is believed that the use of a linear shock cell model is sufficient. The development of such a model will be discussed next. The results of the model is then used in Sec. III to predict the screech tone frequency jet Mach number relation. Comparisons with experimental measurements are carried out. The experimental measurements involved jets from single-bevelled nozzles, double-bevelled nozzles, and regular nozzles. Both convergent and convergent-divergent nozzles are included.

## II. Shock Cell Structure and Screech Frequencies

### A. Physical Model

Let us consider the shock cell structure of a rectangular jet from a single-bevelled rectangular nozzle. Figure 5 shows the plan view of such a jet. For simplicity, we will use a vortex sheet jet model as in the work of Tam.[12] We will assume that the jet Mach number $M_j$ is such that the bevelled angle $\beta$ is larger than the Mach angle $\mu$. When this is true, the disturbances generated by the upstream nozzle side wall would not reach the inside of the nozzle. That is, all of the flow disturbances produced by the boundary discontinuities at the nozzle exit are confined within the jet flow.

For weak shock cells, the shock structure disturbances are governed by the linearized equations of motion. On following Tam,[12]

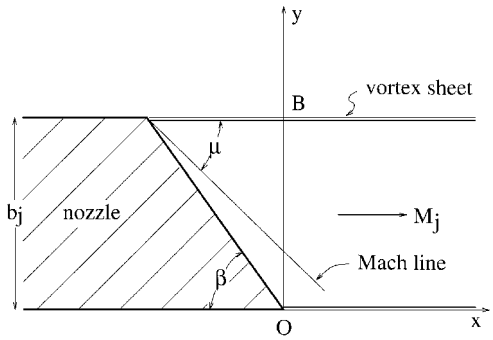


**Fig. 5 Top view of a vortex sheet jet from a single-bevelled rectangular nozzle.**

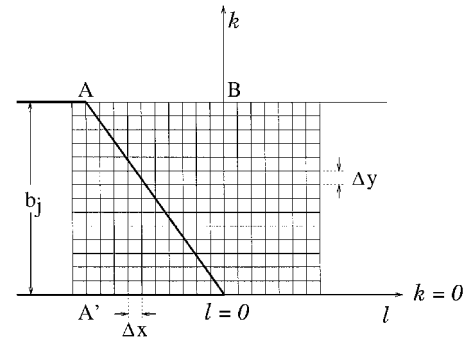


**Fig. 6 Computation domain with mesh size $\Delta x$ and $\Delta y$.**

it is straightforward to find that the pressure $p$ of the shock cells satisfies the equation

$$\nabla^2 p - M_j^2 \frac{\partial^2 p}{\partial x^2} = 0 \tag{10}$$

On the boundaries of the jet (see Fig. 5), the pressure balance boundary condition across the vortex sheet must be satisfied. That is, at $y = 0$, $y = b_j$, $z = 0$, and $z = h_j$,

$$p = 0 \tag{11}$$

Equation (10) and boundary condition (11), as shown by Tam,[12] form an eigenvalue problem that determines the mode shapes and axial wave number of the shock cell or waveguide modes of the jet. The shock cells are formed by a linear combination of these modes according to the linear model. The amplitudes of the shock cell, however, are determined by the initial conditions at the nozzle exit. Thus, the main difference between the shock cells of a rectangular jet with a straight exit and that of a bevelled exit primarily lies on the initial conditions (both have the same eigenmodes). The result is that for a jet with a straight exit the lowest-order mode is most dominant, whereas for a bevelled nozzle the higher-order modes are more dominant.

At the nozzle exit, $y = -z \tan\beta$, both $p$ and $\partial p/\partial x$ are prescribed. These are the initial conditions determined by the supersonic flow upstream (inside the nozzle). For a convergent nozzle, a simple model of the initial condition is

$$p = \Delta p \text{ (const)} \tag{12}$$

$$\frac{\partial p}{\partial x} = 0 \tag{13}$$

For convergent-divergent nozzles with straight side walls, Tam and Reddy[19] have pointed out that a second set of shock cells would be generated at the nozzle throat. Thus, the pressure distribution at the nozzle exit cannot be constant. Therefore, Eqs. (12) and (13) would not be appropriate for these types of nozzles.

### B. Numerical Solution

The initial boundary value problem (10–13) can be solved relatively easily if the solution is first expanded as a Fourier series in $z$. That is, let

$$p(x, y, z) = \sum_{m=1}^{\infty} \hat{p}_m(x, y) \sin\left(\frac{m\pi z}{h_j}\right) \tag{14}$$

On substitution of Eq. (14) into Eq. (10), the governing equation for $\hat{p}_m(x, y)$ is found to be

$$(M_j^2 - 1)\frac{\partial^2 \hat{p}_m}{\partial x^2} - \frac{\partial^2 \hat{p}_m}{\partial y^2} + \frac{m^2\pi^2}{h_j^2}\hat{p}_m = 0 \tag{15}$$

The boundary conditions from Eq. (11), at $y = 0$ and $y = b_j$, are

$$\hat{p}_m = 0 \tag{16}$$

On expanding Eqs. (12) and (13) in Fourier series of $\sin(m\pi z/h_j)$, it is straightforward to find that the initial conditions at the nozzle exit, $y = -x \tan\beta$, are

$$\hat{p}_m = (2/m\pi)(1 - \cos m\pi)\Delta p \tag{17}$$

$$\frac{\partial \hat{p}_m}{\partial x} = 0 \tag{18}$$

We solve Eq. (15), boundary condition (16), and initial conditions (17) and (18) by the finite difference method. To keep the order of the finite difference equations the same as the order of the original partial differential equation (15), we choose to approximate the spatial derivatives by second-order central differences. One principal reason for using a second-order finite difference approximation instead of a higher-order scheme is that the number of initial and boundary conditions for the resulting finite difference equation is identical to those of the original partial differential equation problem. Had a higher-order scheme been used, extra initial and boundary conditions must be imposed to obtain a unique solution. Then a way must be found to impose these extra conditions so that they have no effect on the numerical results. With respect to a mesh of spacing $\Delta x$ and $\Delta y$ (as shown in Fig. 6), the discretized form of Eq. (15) is

$$(M_j^2 - 1)\frac{(\hat{p}_{\ell+1,k} - 2\hat{p}_{\ell,k} + \hat{p}_{\ell-1,k})}{\Delta x^2} - \frac{(\hat{p}_{\ell,k+1} - 2\hat{p}_{\ell,k} + \hat{p}_{\ell,k-1})}{\Delta y^2} + \frac{m^2\pi^2}{h_j^2}\hat{p}_{\ell,k} = 0 \tag{19}$$

where $(\ell, k)$ are the mesh indices in the $x$ and $y$ directions. Equation (19) may be rewritten in the following form so that the value of $\hat{p}_{\ell+1,k}$ may be computed once its values at the last two columns, $\ell$ and $\ell - 1$, are known:

$$\hat{p}_{\ell+1,k} = \left(\frac{\Delta x}{\Delta y}\right)^2 \frac{1}{M_j^2 - 1}(\hat{p}_{\ell,k+1} + \hat{p}_{\ell,k-1}) + \left[2 - \frac{m^2\pi^2}{h_j^2} \times \frac{(\Delta x)^2}{M_j^2 - 1} - 2\left(\frac{\Delta x}{\Delta y}\right)^2 \frac{1}{M_j^2 - 1}\right]\hat{p}_{\ell,k} - \hat{p}_{\ell-1,k} \tag{20}$$

Suppose $\Delta y = b_j/K$, where $K$ is a large integer. Then Eq. (20) is valid for $1 \le k \le K - 1$.

Boundary conditions (16) yield

$$\hat{p}_{\ell,0} = \hat{p}_{\ell,K} = 0 \tag{21}$$

To ensure that the computed solution satisfies initial conditions (17) and (18) at the nozzle exit, a simple way is to start calculating the solution using Eq. (20) at the column $AA'(\ell = -N)$ (as shown in Fig. 6). We set

$$\hat{p}_{-N,k} = \hat{p}_{-(N+1),k} = (2/m\pi)(1 - \cos m\pi)\Delta p \tag{22}$$

and use Eq. (20) to march the solution in the $x$ direction. As soon as the value of $\hat{p}_{\ell,k}$ at a new $\ell$ column (at the first step, this will be $\ell = -N + 1$) is found, all of the values of $\hat{p}_{\ell,k}$ at mesh points that lie inside the nozzle are reset to $2/m\pi(1 - \cos\pi)\Delta p$. This ensures

that at the nozzle exit the slope in the $x$ direction is zero and also that the pressure there is equal to the right-hand side of Eq. (17). The marching process is to be continued until $\ell > 0$ is reached.

Finite difference equation (20) is computationally unstable unless a small value of $\Delta x$ is used. The stability requirement of Eq. (20) can be established by performing a standard Von Neumann analysis. Let

$$\hat{p}_{\ell,k} = \sigma^{\ell} e^{i\lambda k} \tag{23}$$

Substitution of Eq. (23) into Eq. (20) leads to the following equation for $\sigma$:

$$\sigma^2 - Q\sigma + 1 = 0 \tag{24}$$

where

$$Q = \left(\frac{\Delta x}{\Delta y}\right)^2 \frac{2}{M_j^2 - 1}(\cos\lambda - 1) + 2 - \frac{m^2\pi^2}{h_j^2}\frac{(\Delta x)^2}{M_j^2 - 1} \tag{25}$$

The roots of Eq. (24) are

$$\sigma_{\pm} = \tfrac{1}{2}[Q \pm (Q^2 - 4)^{\frac{1}{2}}] \tag{26}$$

One of the roots of Eq. (26) will have a magnitude greater than unity unless $\sigma_{\pm}$ are complex conjugates of each other, in which case $|\sigma_{\pm}| = 1$. The computation scheme is, therefore, stable if $Q^2 < 4$. This yields

$$-4 < \left(\frac{\Delta x}{\Delta y}\right)^2 \frac{2}{M_j^2 - 1}(\cos\lambda - 1) - \frac{m^2\pi^2}{h_j^2}\frac{(\Delta x)^2}{M_j^2 - 1} < 0 \tag{27}$$

The right-side inequality of Eq. (27) is always satisfied. The left-side inequality would be satisfied for all $\lambda$ provided

$$\left(\frac{\Delta x}{\Delta y}\right)^2 \frac{4}{M_j^2 - 1} + \frac{m^2\pi^2}{h_j^2}\frac{(\Delta x)^2}{M_j^2 - 1} < 4$$

Thus, numerical stability is assured if $\Delta x$ is taken to be

$$\Delta x < \frac{(M_j^2 - 1)^{\frac{1}{2}}\Delta y}{[1 + (m^2\pi^2/4)(\Delta y/h_j)^2]^{\frac{1}{2}}} \tag{28}$$

In the present numerical computation, the step size $\Delta x$ used is always smaller than that given by the right-hand side of Eq. (28).

### C. Waveguide Modes of the Shock Cell Structure

In the region of the jet downstream of the $y$ axis at $\ell = 0$, the shock cell solution can again be expanded in terms of the waveguide modes of the jet flow as in Eq. (3). In this case, $\hat{p}_m(x, y)$ may be written in the form

$$\hat{p}_m(x, y) = \sum_{n=1}^{\infty} \sin\left(\frac{n\pi y}{b_j}\right)[A_{nm}\cos(k_{nm}x) + B_{nm}\sin(k_{nm}x)] \tag{29}$$

The coeffcients $A_{nm}$ and $B_{nm}$ are to be determined by joining expansion (29) smoothly to the numerical solution at a location, e.g., at $\ell = L\ (L > 0)$. The joining conditions are the continuity of $\hat{p}_m$ and $\partial\hat{p}_m/\partial x$. On replacing integrals by appropriate sums (the numerical solution is in discretized form), it is straightforward to find from the joining conditions that the values of $A_{nm}$ and $B_{nm}$ are given by

$$A_{nm} = \frac{2\Delta y}{k_{nm}b_j}\left[k_{nm}\cos(k_{nm}L\Delta x)\sum_{k=0}^{K}\hat{p}_{L,k}\sin\left(\frac{n\pi k\Delta y}{b_j}\right) - \sin(k_{nm}L\Delta x)\sum_{k=0}^{K}\frac{1}{2\Delta x}(\hat{p}_{L+1,k} - \hat{p}_{L-1,k})\sin\left(\frac{n\pi k\Delta y}{b_j}\right)\right] \tag{30}$$

$$B_{nm} = \frac{2\Delta y}{k_{nm}b_j}\left[k_{nm}\sin(k_{nm}L\Delta x)\sum_{k=0}^{K}\hat{p}_{L,k}\sin\left(\frac{n\pi k\Delta y}{b_j}\right) + \cos(k_{nm}L\Delta x)\sum_{k=0}^{K}\frac{1}{2\Delta x}(\hat{p}_{L+1,k} - \hat{p}_{L-1,k})\sin\left(\frac{n\pi k\Delta y}{b_j}\right)\right] \tag{31}$$

The amplitude of the $(m, n)$ waveguide mode is

$$C_{nm} = (A_{nm}^2 + B_{nm}^2)^{\frac{1}{2}} \tag{32}$$

### D. Screech Frequencies

Beyond the most downstream edge of the nozzle, the shock cell structure is quasiperiodic. This is the region where the feedback acoustic waves of the screech feedback loop are generated. The physical situation is very similar to that of a jet with a regular straight nozzle exit. The major difference lies in that the dominant waveguide modes that make up the quasiperiodic shock cell structure are not necessarily the lowest-order modes. Moreover, it is possible that more than one mode is dominant. As far as the screech tone feedback loop is concerned, the weakest-link theory is still applicable. However, we expect the resulting screech tones to be more complex. This is because they are related to the higher-order modes; also, more than one feedback loop may be operating at the same time. On following Tam,[12] the screech frequencies can be calculated by replacing $\kappa$ in Eq. (1) by $k_{nm}$ given by Eq. (5). For a large aspect ratio jet ($b_j \gg h_j$), only the $m = 1$ modes are relevant. On restricting our consideration to the $m = 1$ modes, we obtain

$$f_n = \frac{0.55u_j}{2\pi[1 + (0.55u_j/a_\infty)]}\left(\frac{n^2}{b_j^2} + \frac{1}{h_j^2}\right)^{\frac{1}{2}}\frac{\pi}{(M_j^2 - 1)^{\frac{1}{2}}} \tag{33}$$

where $n = 1, 2, 3, \ldots$.

## III. Comparisons with Experiments

Detailed variations of the screech tone frequencies with jet Mach number for an aspect ratio 5 jet have been measured by Raman.[10] In this section, we will compare the frequencies of these measured data with formula (33).

In the experiments of Raman,[10] six rectangular nozzles were used. Three were convergent nozzles and the other three were convergent-divergent (C-D) nozzles. In each family of nozzles, one has a regular straight exit geometry, the second has a single-bevelled geometry, and the third has a double-bevelled geometry. The dimensions of these nozzles were given in the works of Rice and Raman.[5,6] The variation of the screech tone frequencies with fully expanded jet Mach number for each nozzle was measured. However, because more effort was spent on the C-D nozzles, only data related to them were reported. In addition to screech frequencies, the spanwise phase difference and transverse phase difference of the screech tones were also measured. According to the phase information, Raman[10] was able to separate the screech tones into different modes.

Figure 7 shows the measured screech tone frequencies as a function of the jet Mach number for the supersonic jet from the single-bevelled convergent rectangular nozzle. The data do not seem to form a continuous curve. There are frequency jumps at several jet Mach numbers. Also shown are the screech frequencies of formula (33) with spanwise mode number $n = 1, 2, 3$, and 4. As can be seen, the data correlate well with the theoretical frequency curves over the entire range of measured Mach numbers. Figure 8 shows a comparison of the measured screech frequencies and the frequencies of formula (33) for rectangular jets from the double-bevelled convergent nozzle. The screech frequencies agree well with the $n = 5$ and 6 frequency curves.

Figure 9 shows the variation of the screech frequency with Mach number for the supersonic jet from the C-D rectangular nozzle with a regular exit geometry. Based on his spanwise phase data, Raman[10] was able to identify three distinct screech modes. Their frequencies fit very well with the frequencies of the $n = 1$, 3, and 5 modes of formula (33). Figure 10 provides the measured screech frequency jet Mach number relation of the supersonic jet from the single-bevelled C-D rectangular nozzle. According to the phase data, there are three modes, i.e., modes I, IIIA, and IIIB. Also shown are the screech frequency curves for $n = 1, 2, 3$, and 4 modes according to formula (33). The data appear to agree well with the frequency curves of the $n = 1$, 2, and 4 modes. Finally, Fig. 11 shows the measured screech frequency variation with jet Mach number of the supersonic jet from the C-D double-bevelled rectangular nozzle. Two modes have been identified. Their frequencies are in

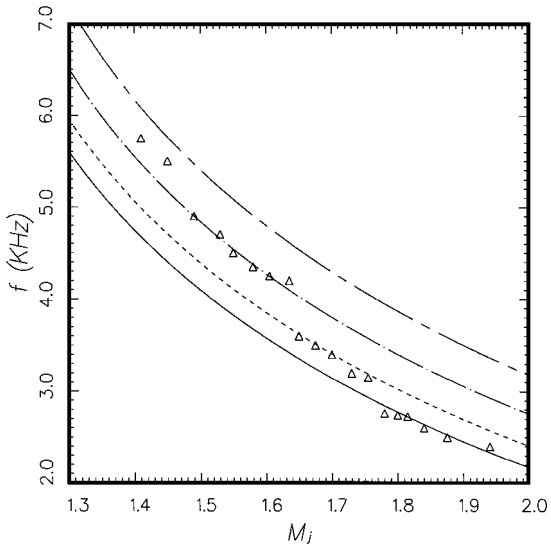


**Fig. 7 Variation of the screech frequencies with fully expanded jet Mach number for a supersonic jet from a convergent rectangular nozzle with aspect ratio = 5, single-bevelled exit geometry: △, measurements.[10] Equation (33): ——, $n$ = 1; – – –, $n$ = 2; – . –, $n$ = 3; and – - –, $n$ = 4.**

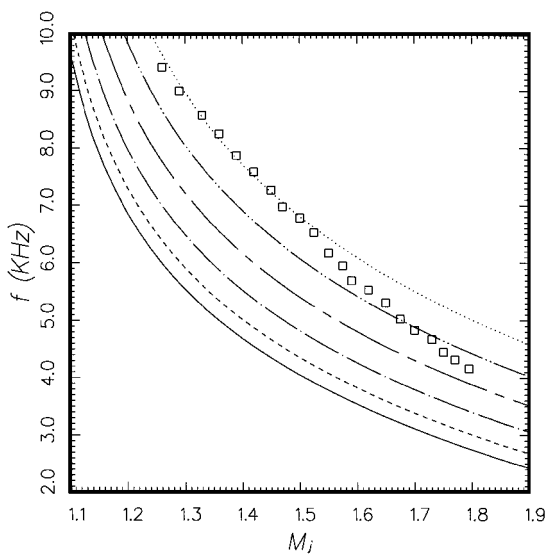


**Fig. 8 Variation of the screech frequencies with fully expanded jet Mach number for a supersonic jet from a convergent rectangular nozzle with aspect ratio = 5, double-bevelled exit geometry: □, measurements.[10] Equation (33): ——, $n$ = 1; – – –, $n$ = 2; – . –, $n$ = 3; – - –, $n$ = 4; – . . –, $n$ = 5; and . . . , $n$ = 6.**

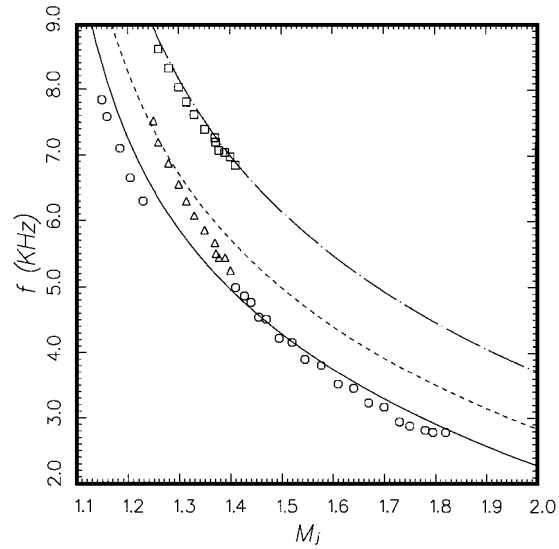


**Fig. 9 Variation of the screech frequencies with fully expanded jet Mach number for a supersonic jet from a convergent-divergent rectangular nozzle with aspect ratio = 5, $M_d$ = 1.4, and regular exit geometry. Measurements[10]: ○, mode I-1; △, mode I-2; and □, mode II. Equation (33): ——, $n$ = 1; – – –, $n$ = 3; and – . –, $n$ = 5.**

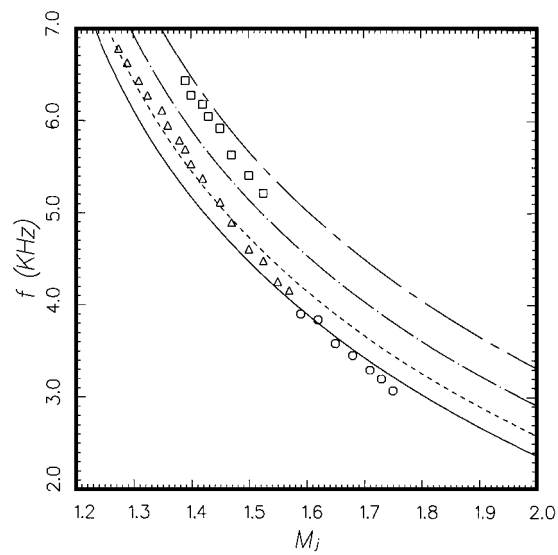


**Fig. 10 Variation of the screech frequencies with fully expanded jet Mach number for a supersonic jet from a convergent-divergent rectangular nozzle with aspect ratio = 5, $M_d$ = 1.4, and single-bevelled exit geometry. Measurements[10]: ○, mode I; △, mode III-A; and □, mode III-B. Equation (33): ——, $n$ = 1; – – –, $n$ = 2; – . –, $n$ = 3; and – - –, $n$ = 4.**

reasonable agreement with the $n = 6$ and 7 frequency curves of formula (33).

Formula (33) predicts many screech frequency bands. However, not all of the tones of the frequency bands are excited. We believe that the selection of the excited frequencies is determined largely by two factors. They are the spatial growth rates of the instability waves of the jet flow and the strength of the waveguide modes of the shock cell structure. Here, we will examine, by means of the shock cell model given earlier, how the strength of the waveguide modes influences tone selection, as well as the frequency jumps in the data of Fig. 7. For this purpose, the amplitudes of the waveguide modes corresponding to $m = 1$, $n = 1$, 2, 3, and 4 were calculated by the marching scheme (20). In the numerical computation $K$ was taken to be 8000. The size of the marching step $\Delta x$ was chosen to be smaller than that given by Eq. (28). The solution was marched from the starting line $AA\prime$ in Fig. 6 to a line downstream of the $y$ axis before the coefficients $A_{n1}$, $B_{n1}$, and $C_{n1}$ were evaluated according to Eqs. (30–32). To check the accuracy of the numerical results, each computation was marched farther downstream. At this new location, the amplitude $C_{n1}$ was again determined. It was found in every case that the two calculated values of $C_{n1}$ agreed to at least three significant figures. This offers assurance that the numerical results are accurate.

Figure 12 shows the computed waveguide mode amplitude $C_{n1}$, $n = 1$, 2, 3, 4, of the shock cell structure for a single-bevelled convergent rectangular nozzle used in the experiment of Raman.[10] In the computation, $\Delta p$ was set equal to unity for convenience. At a low supersonic Mach number, the dominant mode is the $n = 4$ mode. As the Mach number increases, the dominant mode shifts to $n = 3$, then $n = 2$, and finally at $M_j > 2$ the $n = 1$ mode becomes the most dominant. This trend correlates well with the measured data in Fig. 7.

If the shock cell strength is the only factor that determines the dominant screech tone, then the information in Fig. 12 can be used to predict the locations of the frequency jumps observed in Fig. 7. Let us assume that a shift in the excited frequency is possible when the waveguide mode amplitudes of the adjacent bands are within 15%

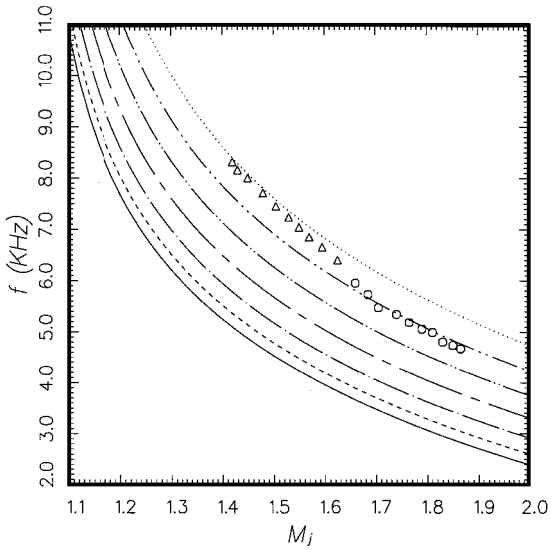


**Fig. 11 Variation of the screech frequencies with fully expanded jet Mach number for a supersonic jet from a convergent-divergent rectangular nozzle with aspect ratio = 5 and double-bevelled exit geometry. Measurements[10]: ○ mode I and △ mode II. Equation (33): – – –, $n = 6$ and . . . , $n = 7$.**

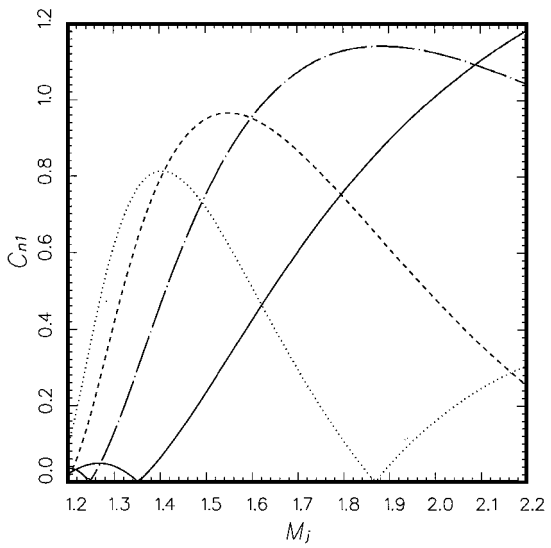


**Fig. 12 Amplitude of the waveguide modes of the shock cell structure in the plume of a supersonic jet downstream of a convergent single-bevelled rectangular nozzle with aspect ratio = 5: ——, $C_{11}$; – .–, $C_{21}$; – – –, $C_{31}$; and . . . , $C_{41}$.**

of each other. Figure 13 shows the mode switching Mach number or the expected locations of frequency jumps. The predicted locations for mode switching from $n = 4$ to $n = 3$ and from $n = 3$ to $n = 2$ (indicated by arrows) are in fair agreement with measurements. The switch from $n = 2$ to $n = 1$ mode takes place around $M_j = 1.75$, whereas the calculated value falls around $M_j = 2.0$. We believe that the discrepancy is solely because the effect of the growth rate of the instability waves has not been considered. Despite this discrepancy, the good overall agreement leaves little doubt that the strength of the waveguide modes of the shock cell structure plays a crucial role in the selection of the observed screech tones.

## IV. Summary

The screech tone frequency patterns of supersonic jets from bevelled rectangular nozzles and C-D nozzles with straight side walls are quite complex. It is suggested that these tones are related to the higher-order waveguide modes of the shock cell structure in the jet plume. By using a simple vortex sheet jet model to calculate the linear shock cell waveguide modes of the jet and then calculate the

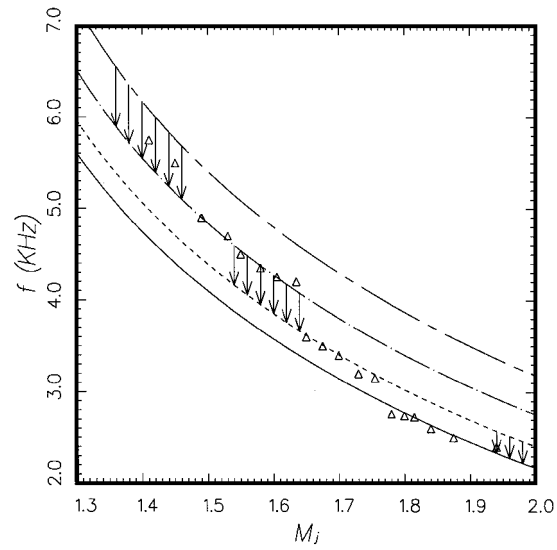


**Fig. 13 Mode-switching Mach numbers: ↓↓↓↓, based on computed waveguide mode amplitudes.**

screech frequencies by the axial wave number of these modes, it is shown that the predicted screech frequency curves agree well with all of the measured data. The good agreement provides strong support for the waveguide mode concept of the shock cell structure and the weakest link feedback theory of jet screech.

The shock cell structure is modeled by a superposition of waveguide modes of the jet flow. This modal decomposition is unquestionably at odds with the concept of shock cells with sharp discontinuities. One major difference between the two models is that there can only be one screech tone associated with a shock cell structure with sharp discontinuities (there is only one shock cell length). On the other hand, there can be more than one screech tone according to the waveguide model. We have found good agreement between the screech frequencies predicted by the waveguide shock cell model and experimental measurements. Furthermore, Raman[10] has shown experimentally that two screech tones can exist simultaneously. Thus, there is no question that a waveguide model representation of the shock cells of a supersonic jet is valid. However, the authors believe that the range of validity is limited only to the moderately imperfectly expanded Mach number range of the nozzle. For highly imperfectly expanded jets, nonlinear effects dominate the formation of the shock cell structure. In this case, the structure is made up of sharp shocks. It follows, therefore, for highly imperfectly expanded jets there would only be a single screech tone. This appears to be consistent with all of the screech tone data available in the literature at the present time.

## Acknowledgment

The work of the first two authors was supported in part by NASA Langley Research Center Grant NAG 1-1776.

## References

[1]Powell, A., "On the Noise Emanating from a Two-Dimensional Jet Above the Critical Pressure," *Aeronautical Quarterly*, Vol. 4, 1953, pp. 103–122.

[2]Hammitt, A. G., "The Oscillation and Noise of an Overpressure Sonic Jet," *Journal of the Aerospace Sciences*, Vol. 28, 1961, pp. 673–680.

[3]Krothapalli, A., Hsia, Y., Baganoff, D., and Karamcheti, K., "The Role of Screech Tones on Mixing of an Underexpanded Rectangular Jet," *Journal of Sound and Vibration*, Vol. 106, 1986, pp. 119–143.

[4]Rice, E. J., and Taghavi, R., "Screech Noise Source Structure of a Supersonic Rectangular Jet," AIAA Paper 92-0503, Jan. 1992.

[5]Rice, E. J., and Raman, G., "Mixing Noise Reduction for Rectangular Supersonic Jets by Nozzle Shaping and Induced Screech Mixings," AIAA Paper 93-4322, Oct. 1993.

[6]Rice, E. J., and Raman, G., "Supersonic Jets from Bevelled Rectangular Nozzles," American Society of Mechanical Engineers, ASME Paper 93-WA/NCA-26, 1993.

[7]Raman, G., and Rice, E. J., "Instability Modes Excited by Natural Screech Tones in a Supersonic Rectangular Jet," *Physics of Fluids*, Vol. 6, Dec. 1994, pp. 3999–4008.

[8]Umeda, Y., and Ishii, R., "Oscillation Modes of Underexpanded Jets Issuing from Square and Equilateral Triangular Nozzles," *Journal of the Acoustical Society of America*, Vol. 95, 1994, pp. 1853–1857.

[9]Walker, S. H., Gordeyer, S. V., and Thomas, F. O., "A Wavelet Transform Analysis Applied to Unsteady Jet Screech Resonance," *Proceedings ASME/JSME Fluids Engineering and Laser Anemonetry Conference and Exhibition* (Hilton Head, SC), American Society of Mechanical Engineers, New York, 1995, pp. 103–108.

[10]Raman, G., "Screech Tones from Rectangular Jets with Spanwise Oblique Shock-Cell Structures," AIAA Paper 96-0643, Jan. 1996.

[11]Tam, C. K. W., Jackson, J. A., and Seiner, J. M., "A Multiple-Scales Model of the Shock Cell Structure of Imperfectly Expanded Supersonic Jets," *Journal of Fluid Mechanics*, Vol. 153, 1985, pp. 123–149.

[12]Tam, C. K. W., "The Shock-Cell Structure and Screech Tone Frequencies of Rectangular and Non-Axisymmetric Supersonic Jets," *Journal of Sound and Vibration*, Vol. 121, 1988, pp. 135–147.

[13]Morris, P. J., Bhat, T. R. S., and Chen, G., "A Linear Shock Cell Model for Jets of Arbitrary Exit Geometry," *Journal of Sound and Vibration*, Vol. 132, 1989, pp. 199–211.

[14]Tam, C. K. W., "Broadband Shock Associated Noise of Moderately Imperfectly Expanded Supersonic Jets," *Journal of Sound and Vibration*, Vol. 140, 1988, pp. 55–71.

[15]Tam, C. K. W., "Broadband Shock Associated Noise from Supersonic Jets Measured by a Ground Observer," *AIAA Journal*, Vol. 30, No. 10, 1992, pp. 2395–2401.

[16]Tam, C. K. W., "Supersonic Jet Noise," *Annual Review of Fluid Mechanics*, Vol. 27, 1995, pp. 17–43.

[17]Tam, C. K. W., Seiner, J. M., and Yu, J. C., "Proposed Relationship between Broadband Shock Associated Noise and Screech Tones," *Journal of Sound and Vibration*, Vol. 110, 1986, pp. 309–321.

[18]Harper-Bourne, M., and Fisher, M. J., "The Noise from Shock Waves in Supersonic Jets," *Proceedings of the AGARD Conference on Noise Mechanisms*, No. 131, Brussels, Belgium, 1973.

[19]Tam, C. K. W., and Reddy, N. N., "Prediction Method for Broadband Shock Associated Noise from Supersonic Rectangular Jets," *Journal of Aircraft*, Vol. 33, No. 2, 1996, pp. 298–303.

S. Glegg
*Associate Editor*